X-615-68-442
PREPRINT

TYPE III RADIO BURSTS IN THE OUTER CORONA

J. K. ALEXANDER
H. H. MALITSON
R. G. STONE

NOVEMBER 1968

GSFC
GODDARD SPACE FLIGHT CENTER
GREENBELT, MARYLAND

X-615-68-442

TYPE III RADIO BURSTS IN THE OUTER CORONA

J. K. Alexander, H. H. Malitson, and R. G. Stone

Laboratory for Space Sciences

NASA Goddard Space Flight Center

Greenbelt, Maryland

TYPE III RADIO BURSTS IN THE OUTER CORONA

J. K. Alexander, H. H. Malitson, and R. G. Stone

Laboratory for Space Sciences

ABSTRACT

Type III solar radio bursts observed from 3.0 to 0.45 MHz with the ATS-II satellite over the period April-October 1967 have been analyzed to derive two alternative models of active region streamers in the outer solar corona. Assuming that the bursts correspond to radiation near the electron plasma frequency, "pressure equilibrium" arguments lead to streamer Model I in which the streamer electron temperature derived from collision damping time falls off much more rapidly than in the "average" corona and the electron density is as much as 25 times the average coronal density at heights of 10 to 50 solar radii ($R_\odot$). In Model II the streamer electron temperature is assumed to equal the average coronal temperature, giving a density enhancement which decreases from a factor of 10 close to the Sun to less than a factor of two at large distances (>1/4 A.U.). When the burst frequency drift is interpreted as resulting from the outward motion of a disturbance that stimulates the radio emission, Model I gives a constant velocity of about 0.35c for the exciting disturbance as it moves to large distances, while with Model II, there is a decrease in the velocity to less than 0.2c beyond 10 $R_\odot$.

INTRODUCTION

Information about the density and temperature structure of the corona has come from the use of widely varying techniques. Optical measurements during and outside of solar eclipse have yielded data out to 30 $R_\odot$, but these can be reliably translated into density and temperature profiles only out to about 10 $R_\odot$ (Newkirk, 1967). Wild and his colleagues (Wild et al., 1959; Weiss, 1963) used interferometric positional measurements of Type II and III bursts at metric wavelengths to derive densities above active regions, presumably representative of active region streamers. Further work has been done at decametric wavelengths (e.g., Malitson and Erickson, 1966) to give a density profile out to about 3 $R_\odot$, but extension of this method to greater heights in the corona depends on observations from above the ionosphere. Beyond 10 $R_\odot$, except for in situ measurements of density and temperature near the Earth's orbit, the only applicable observations to date are those of coronal occultations of discrete radio sources and of low frequency radio bursts by means of satellites.

Although observations of scintillations of discrete radio sources due to density fluctuations in the corona (e.g., those of Erickson, 1964) are good indicators of the shape of the corona from 10 to 80 $R_\odot$, the derivation of a density profile involves several unverified assumptions about the nature and distribution of the irregularities. Until more is known about the small-scale structure of the corona, the occultation method will have

limited applicability. Meanwhile, the study of solar radio bursts from above the earth's ionosphere at hectometric and kilometric wavelengths is beginning to fill in the gaps in present knowledge of the physical properties of the corona. The results of Slysh (1967) for Type III bursts at 1 MHz and 200 kHz, of Hartz (1968) over the range 15 MHz-600 kHz, and those contained in this report suggest a high-density, low-temperature model for coronal active region streamers out to about 50 $R_\odot$. An alternative model with higher temperatures and moderate density enhancements over the background is also possible.

TYPE III BURST OBSERVATIONS

The observations to be discussed here were obtained with the ATS-II satellite, which was launched April 6, 1967 into an elliptical, 28° inclination orbit with an 11,000 km apogee and 180 km perigee. Since details of the ATS-II radio astronomy experiment have been presented elsewhere (Stone et al., 1968; Somerlock and Krustins, 1968) we will only summarize the salient features of the instrument. In brief, it consists of a 76-meter dipole antenna which is connected through a pair of high impedance pre-amplifiers to a Ryle-Vonberg type comparison radiometer. The radiometer is stepped through six discrete frequencies between 0.45 and 3.00 MHz once every 40 sec. The pre-detection bandwidth is 40 kHz, and the post-detection integration time constant is 1 sec. Approximately 1130 hours of measurements were obtained between launch date and

October 23, 1967, when routine spacecraft operations were terminated. About 40% of the data showed evidence of "contamination" due to terrestrial noise bursts (Bauer and Stone, 1968) and other local phenomena. During the remaining 680 hours available for solar measurements we have observed over fifty burst events which clearly exhibit the rapid frequency drift pattern characteristic of Type III solar bursts. There were an additional fifty burst events observed that we would class as "probable" Type III's. Since our experiment operated on a 50% duty cycle (i.e., 10 min. on - 10 min. off), thi corresponds tc an occurrence frequency of about 0.15-0.3 bursts per hour as compared with 1 burst per hour reported for Type III's at decametric wavelengths for a comparable level of solar activity. This apparent decrease is probably due in part to sensitivity limitations arising from spacecraft RFI levels. Very recent measurements from the first Radio Astronomy Explorer satellite tend to confirm this explanation, and show a large number of Type III bursts in the 1 MHz region. Data used for analysis of solar bursts were confined to times when the satellite was above 5000 km.

The distribution of bursts with frequency (Figure 1) suggests an interesting trend. Of all those bursts observed at 2.2 MHz, only about 80% extend to 0.7 MHz and 28-68% are found to go to 0.45 MHz. (The large uncertainty is due to a deficiency of data at 0.45 MHz which became more serious during the final weeks.) Part of this effect may be due to

screening of the lower frequencies by the ionosphere, but when the analysis is confined to bursts observed at altitudes above 9000 km (the 0.45 MHz plasma level is below 7000 km) only 12-36% of those bursts observed at 2.2 MHz extend down to 0.45 MHz. To investigate the possible influence of coronal propagation effects on the burst-frequency distribution we sorted all bursts observed according to the heliocentric latitude and longitude of the solar flare most likely associated with the bursts. Flare information was obtained from the monthly "Solar-Geophysical Data" reports from ESSA in Boulder, Colorado. Although there is some evidence of a propagation effect reflected by a decrease in the number of low frequency bursts associated with flares more than 45° from the center of the solar disk, the distribution of all bursts associated with active centers within 45° of the center still clearly shows a drop-off in the number of bursts that extend down to 0.45 MHz. In other words, it appears that all Type III's do not drift to indefinitely lower frequencies.

Several examples of Type III bursts observed with the ATS experiment are shown in Figure 2. Since the antenna was shared with another experiment on the satellite, radio noise measurements were obtained for a period of ten minutes, and then the experiment was off during alternate ten minute periods. The radiometer stepped through six frequencies - 0.45, 0.7, 1.1, 1.6, 2.2 and 3.0 MHz - in 40 seconds. Although this sampling rate is not sufficiently fast to show the time structure of the

bursts in detail, the abrupt onset, rapid drift from high to low frequencies, and the approximately exponential decay common to Type III bursts are apparent in the examples shown in Figure 2. Note also that there is a tendency for both the rise times and the decay times of the bursts to increase as frequency decreases.

For each burst, we have measured the time taken for the maximum to drift from one frequency to the next lower one. The drift rates derived from these measurements are plotted on Figure 3, along with some results from other investigations. The straight line represents the observations of Hartz (1968) from the Alouette I and II satellites, and the crosses come from a study of University of Colorado radio spectrograph data by Boischot (1967). It should be pointed out that the ATS-II points are based on drift rates of the burst maxima, which are somewhat lower than the drift rates of burst commencement times used by Hartz and Boischot. In our case, burst maximum times gave more consistent results, being relatively insensitive to the level of the background noise above which the burst had to be recognized. The error bars in Figure 3 reflect the uncertainty in estimated drift times due to the relatively slow sampling rate of the experiment.

The decay times (i.e., e-folding times) for all Type III's observed are shown in Figure 4 where we have plotted the average decay time for each frequency. The times vary inversely with frequency from 30 sec at 3 MHz to about 120 sec at 0.45 MHz. The error bars again show the effect of the slow sampling rate.

DERIVATION OF CORONAL STREAMER TEMPERATURE AND DENSITY

Following Boischot, Lee, and Warwick (1960) and others, we can use the burst decay time to estimate the streamer electron temperature. If one assumes that the Type III bursts are due to plasma oscillations at or near the local electron plasma frequency and that electron-ion collisions are primarily responsible for the damping of the oscillations, then the electron temperature is given by

$$T_e = 0.65 \times 10^{-4} \tau^{2/3} f^{4/3} \qquad \text{(Eq. 1)}$$

where τ is the e-folding duration of the burst observed at a radio frequency f (Jaeger and Westfold, 1949). Upon using the decay times shown in Figure 4 in Equation 1, we get electron temperatures which vary systematically from 2.9×10^5 K at 3.0 MHz to 5.4×10^4 K at 0.45 MHz. Similar results are obtained from an equation due to Spitzer (1956) which differs from the above by a constant factor, typically of the order of 4.

In order to apply the temperatures deduced from burst decay times to a model of an active region coronal streamer we must have an independent means of determining the height in the solar corona to which the measured temperatures apply. For that purpose, we assume an equilibrium between the total pressure in a streamer and in the surrounding coronal plasma. That is,

$$2N_s kT_s + B_s^2/8\pi = 2N_a kT_a + B_a^2/8\pi \qquad \text{(Eq. 2)}$$

where N_s, T_s, and B_s refer respectively to the streamer electron density,

temperature, and magnetic field and N_a, T_a, and B_a refer to the same quantities in the "average" corona. The magnetic pressure in the streamer is assumed to be negligibly small, thus eliminating the second term on the left side of the equation. Support for this approach is provided by the model of Sturrock and Smith (1968) based on eclipse observations, in which a streamer is the visible manifestation of a current sheet between two tubes of opposite magnetic flux. The magnetic pressure in the sheet would be zero, therefore making it necessary for the gas pressure alone to balance the total pressure in the surrounding "average" corona.

Next, in order to estimate the streamer density and temperature distribution, we adopt models for the density, temperature, and magnetic field in the average corona, based on presently available data, and then determine the altitude at which Equation 2 is satisfied. For the average corona we have used the electron density model for the solar wind by Whang, Liu, and Chang (1966) which compares well with other equatorial coronal models close to the Sun and with space probe measurements near 1 A.U. The average electron temperature model adopted is similar to that developed by Noble and Scarf (1963) which ranges from 2×10^6 K at one solar radius to about 3×10^5 K at 1 A.U. Finally, we have taken the average coronal magnetic field to vary inversely with the square of the distance from 2.5 gauss at one solar radius to 5 gamma at 1 A.U. (a

figure that also agrees well with space probe measurements). These assumptions lead to the streamer temperature and density models labelled "Model I" in Figu. e 5.

We find that the streamer temperatures fall off much more steeply than in the average coronal model and, when extrapolated to 1 A.U., suggest that if streamers extend that far out they would have temperatures below 10^4 K. The streamer densities are not inconsistent with the model of Malitson and Erickson (1966) for lower altitudes but are enhanced over the average coronal densities by a factor of 20 to 30 at heights of 30 to 50 $R_\odot$. Model I, therefore, is consistent with the results of a similar analysis by Hartz (1968) and suggests a picture of dense, cold streamers.

The streamer model derived above should probably be interpreted as giving a lower limit to electron temperatures and an upper limit to electron densities. It seems likely that there are other damping mechanisms in addition to collisions which will contribute to the burst decay and thereby lead to temperatures which, if calculated on the basis of collisions alone, will be too low. Upon including a finite magnetic pressure term on the streamer side of Equation 2, a given density point is shifted to a lower altitude, thereby reducing the factor by which the streamer density is enhanced over the average coronal density.

To investigate the effect of a higher streamer temperature than that deduced from the decay times we have developed a second model in which

the streamer temperature is taken to be equal to the average coronal temperature at large distances from the Sun. The resulting density distribution using Equation 2 with $T_s = T_a$ is labelled "Model II" in Figure 5. Now the streamer densities are enhanced over the average densities by a factor of 5 at 30 $R_\odot$, and the streamers tend to merge into the surrounding corona at greater distances from the Sun. When extrapolated to 1 A.U., Model II suggests that the streamer would simply appear as a 10 to 20% increase over the average density. To make this density model consistent with the Malitson and Erickson streamer model at low altitudes, we need only include a small streamer magnetic pressure term or allow the streamer temperature to slightly exceed the average temperature close to the Sun.

VELOCITIES OF TYPE III BURSTS

If the Type III bursts are interpreted as being due to plasma oscillations excited at successively higher levels in the corona by a disturbance moving rapidly along a streamer, then the frequency drift rates can be used to determine the velocity of the disturbance. We have used the delay in the times of peak intensity at each observing frequency to calculate velocities for both density models, and the distribution of velocities determined for bursts drifting between 2.2 and 1.1 MHz is shown in Figure 6. Since the radio emission at different frequencies is

postulated to come from different altitudes in the corona, the observed time delays must be corrected for the difference in the light time between the points of origin at each frequency. To do this, we assumed that each burst occurred radially above the most actively flaring region on the disk at the time of the burst. The time correction to be applied to the delay times between two frequencies is then given by

$$t = \frac{(R^2 - 2AR\cos\theta + A^2)^{1/2} - (r^2 - 2Ar\cos\theta + A^2)^{1/2}}{c} \qquad \text{(Eq. 3)}$$

where R, r are the radial distances from the Sun to the points of origin at the two frequencies, θ is the heliocentric angle between the Earth and the source, A is the length of the A.U., and c is the velocity of light. The velocity distributions thus approximately corrected are shown by the dashed histograms in Figure 6. The average velocities are found to fall at 0.3 to 0.35c for density Model I and 0.15 to 0.18c for Model II.

In Figure 7 we have plotted the corrected velocities deduced from the drift times at each frequency as a function of distance for both streamer models. Also shown are velocities deduced from ground-based observations of drift rates at high frequencies all calculated on the basis of the Malitson and Erickson streamer model and velocities calculated from Hartz's drift rates using our density curves for Model I and Model II. In spite of the considerable spread in the high-frequency points and the necessarily large error bars on the low-frequency points, certain trends

are evident in Figure 7. In Model I the average Type III burst velocity is nearly constant out to at least 50 $R_\odot$ at a value of about 0.35c. In Model II the average velocity appears to decrease with distance, from a value of about 0.45c at one solar radius to about 0.15c at 30 $R_\odot$.

DISCUSSION

Streamer temperatures derived by assuming that the decay rate is due entirely to collisional damping are found to fall off as R^{-1}, i.e., far more rapidly than expected for the ambient solar wind. Corrections to account for the finite extent of the exciter or a larger emission bandwidth will only tend to lower the temperature. As suggested by Newkirk (1967) the R^{-1} decrease of temperature might be a consequence of subsonic streamer flow resulting from the choking off of the supersonic solar wind by the high streamer density. Yet there have been no definite space observations showing the existence of such cold, dense streamers extending out to the orbit of the Earth. Furthermore, the assumption that the emission decay is due entirely to collisional damping may be incorrect. For realistic temperatures and exciter velocities, Landau damping is ineffective compared to collisional damping. Since there is no reason to expect that the excited plasma is Maxwellian, it should be possible to obtain significant collisionless damping by proper choice of a distribution function. This point will not be pursued further here. There is also the possibility that the decay is apparent in that the excited plasma spectrum may

shift to longer wavelengths where the emission is not observable. This has been considered by Tsytovich (1966) using nonlinear plasma theory.

Our Model I is used to illustrate the typical streamer characteristics resulting from an energy density balance argument, an ambient solar wind model, and streamer temperatures deduced from damping times. Model II, on the other hand, disregards the temperatures derived from the burst decay and assumes streamer and ambient coronal temperatures are equal. This model was introduced to obtain a somewhat independent determination of exciter velocity. The model has the interesting property that the streamer density enhancement relative to the ambient corona first increases and then slowly decreases to the ambient coronal density value. This type of structure is expected on the basis of more substantive analysis as presented by Pneuman (1968).

The data in Figure 1 suggest that the occurrence probability of Type III bursts apparently decreases with frequency, i.e., with distance. This conclusion is tentative because of the limited sample of bursts available after discarding those not observed near satellite apogee and those with associated flares at large heliocentric angles. Sensitivity limitations of the ATS experiment may also invalidate the occurrence probability analysis. However if the result is valid, the decrease of occurrence probability could be explained by a "thinning out", i.e., decrease in density,

of the streamer at large distances. As the streamer density approaches that of the ambient plasma, the range of angles over which the radio emission can escape will decrease. There is also the possibility that at some distance out, the streamer can no longer contain the exciting mechanism, so that the emission cannot be observed.

An experiment conducted by Slysh (1967b) has introduced an interesting challenge to the hypothesis that emission occurs near the plasma frequency. The approximate positions of bursts at 200 kHz were obtained both from antenna null positions and from lunar occultations observed with the Luna-11 and -12 probes. Slysh found that the bursts occurred at a distance approximately $200\,R_\odot$ from the Sun. The plasma hypothesis would place the 200 kHz level at about $100\,R_\odot$. To account for his observations, Slysh invokes a theory developed by Gailitis and Tsytovich (1964) which gives emission at a frequency well above the local plasma frequency. It is interesting to note that over the frequency range common to the ATS and Luna experiments, the density profile derived by Slysh is essentially in agreeement with the results of Model I.

SUMMARY

Two models of active region coronal streamers at large distances from the Sun have been developed for use in interpreting Type III radio burst observations at low frequencies. The cold, dense streamers pictured in Model I probably represent lower limits to the electron

temperatures and upper limits to the electron densities. Actual streamer parameters probably fall somewhere between these limits and the values given by Model II, in which the streamer temperature remains equal to that of the ambient corona, and the streamer density approaches ambient solar wind density far from the Sun. Direct measurements pertaining to the existence of streamers out to 1 A. U., and the determination of the characteristics of solar radio bursts to kilometric wavelengths would go far toward resolving these questions.

ACKNOWLEDGMENTS

The authors gratefully acknowledge the contributions of C. R. Somerlock and J. Krustins who designed and calibrated the ATS-II radiometer, and J. M. Stockwell and S. Blecher who were responsible for the computer processing of the experimental data.

REFERENCES

Bauer, S. J. and Stone, R. G.: 1968, Nature 218, 1145-1147.

Boischot, A., Lee, R. H., and Warwick, J. W.: 1960, Astrophys. J. 131, 61-67.

Boischot, A.: 1967, Ann. d'Astrophys. 30, 85-91.

Clark, T. A.: 1967, Thesis, University of Colorado.

Elgarøy, Ø. and Rødberg, H.: 1963, Nature 199, 268.

Erickson, W. C.: 1964, Astrophys. J. 139, 1290-1311.

REFERENCES (Continued)

Gailitis, A. and Tsytovich, V. N.: 1964, J. Exptl. Theoret. Phys. (USSR) 46, 1726-1739 (Soviet Phys. JETP 19, 1165-1173).

Hartz, T. R.: 1968, Preprint, "Type III Solar Radio Noise Bursts at Hectometer Wavelengths."

Jaeger, J. C. and Westfold, K. C.: 1949, Australian J. Sci. Res. A2, 322-334.

Malitson, H. H. and Erickson, W. C.: 1966, Astrophys. J. 144, 337-351.

Malville, J. M.: 1962, Astrophys. J. 136, 266-275.

Maxwell, A.: 1965, in The Solar Spectrum (ed. by C. de Jager), D. Reidel, Dordrecht-Holland, 342-397.

Newkirk, G., Jr.: 1967, in Annual Review of Astronomy and Astrophysics 5, 213-266.

Noble, L. M. and Scarf, F. L.: 1963, Astrophys. J. 138, 1169-1181.

Pneuman, G. W.: 1968, Solar Phys. 3, 578-597.

Riihimaa, J. J.: 1963, Ann. Acad. Scient. Fennicae A VI 131, 3-17.

Slysh, V. I.: 1967a, Astronom. Zhurnal 44, 487-489 (Soviet Astronomy-AJ 11, 389-391).

Slysh, V. I.: 1967b, Kosmicheskiye Issledovania 5, 897-910.

Somerlock, C. R. and Krustins, J.: NASA Technical Note D-4634.

Spitzer, L.: 1956, Physics of Fully Ionized Gases, Interscience, New York.

REFERENCES (Continued)

Stone, R. G., Malitson, H. H., Alexander, J. K. and Somerlock, C. R.: 1968, in Structure and Development of Solar Active Regions (ed. by K. O. Kiepenheuer), D. Reidel, Dordrect-Holland, 585-587.

Sturrock, P. A. and Smith, S. M.: 1968, Solar Phys. 5, 87-101.

Tsytovich, V. N.: 1966, Usp. Phys. Nauk 90, 435-489 (1967, Soviet Phys. Uspekhi 9, 805-836).

Weiss, A. A.: 1963, Australian J. Phys. 16, 240-271.

Whang, Y. C., Liu, C. K. and Chang, C. C.: 1966, Astrophys. J. 145, 255-269.

Wild, J. P.: Australian J. Sci. Res. A3, 541-557.

Wild, J. P., Sheridan, K. V. and Neylan, A. A.: 1959, Australian J. Phys. 12, 369-398.

FIGURE CAPTIONS

Figure 1. Percentage of Type III bursts observed at 2.2 MHz that extend to lower frequencies. The burst frequency distribution relative to 2.2 MHz is shown as a function of satellite altitude and heliocentric angle of the associated active region.

Figure 2. Sample portions of ATS-II radiometer data showing Type III bursts. The small brackets along the bottom of each diagram denote the times when Type III bursts were detected by the University of Colorado decametric radio spectrograph.

Figure 3. Change of drift rate of Type III bursts with frequency. The open circles represent ATS-II data. The solid line was derived by Hartz (1968) from Alouette-I and -II satellite data and the crosses are from Boischot's analysis (1967) of data from the radio spectrograph of the University of Colorado.

Figure 4. Variation of the average burst decay time (e-folding time) with frequency.

Figure 5. Models of the variation of electron density and temperature with distance from the center of the Sun for the "average" corona and for active region streamers. Model I streamer temperatures are derived from burst decay times; Model II streamer and "average" temperatures are assumed to be equal.

FIGURE CAPTIONS (Continued)

Figure 6. Distribution of Type III burst exciter velocities derived from the frequency drift times between 2.2 and 1.1 MHz and the Model I and II streamer electron density distributions. Assuming that the disturbance moves radially outward from the associated active region, the dashed histogram shows the effect of correcting for the difference in propagation time from the points of origin at the two frequencies.

Figure 7. Variation of burst exciter velocity with distance from the center of the Sun. For comparison with the ATS data, the broken curves show the velocities derived from Hartz's (1968) drift rates in terms of Models I and II; whereas the numbered points (1- Elgarøy and Rødberg, 1963; 2- Maxwell, 1965; 3- Wild, 1950; 4- Wild et al., 1959; 5- Riihimaa, 1963; 6- Malville, 1962; 7 - Clark, 1967) refer to ground-based drift rate measurements reduced in terms of the Malitson and Erickson (1966) streamer model.

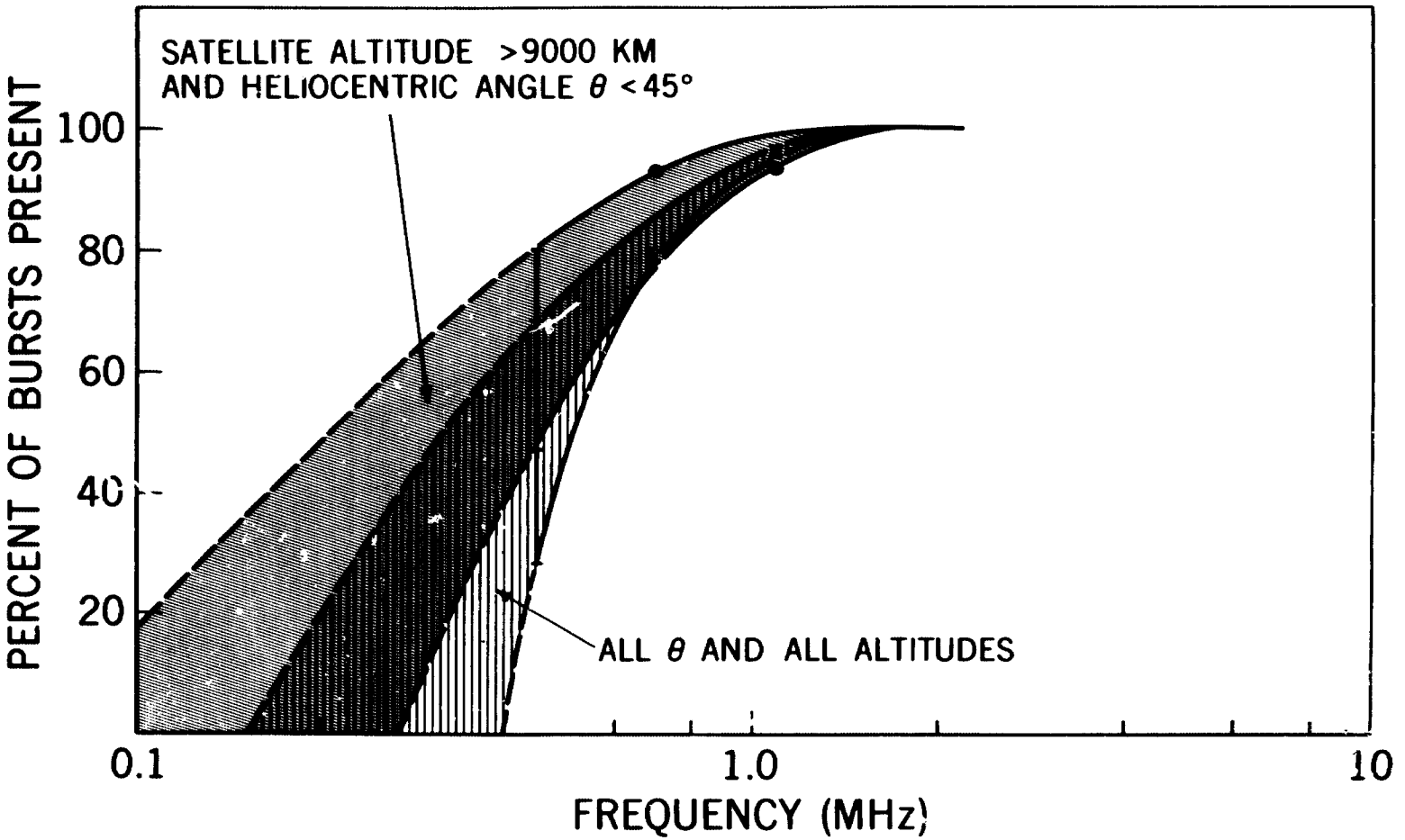
SATELLITE ALTITUDE >9000 KM
AND HELIOCENTRIC ANGLE θ <45°
ALL θ AND ALL ALTITUDES
PERCENT OF BURSTS PRESENT
100
80
60
40
20
0.1
1.0
10
FREQUENCY (MHz)

Figure 1

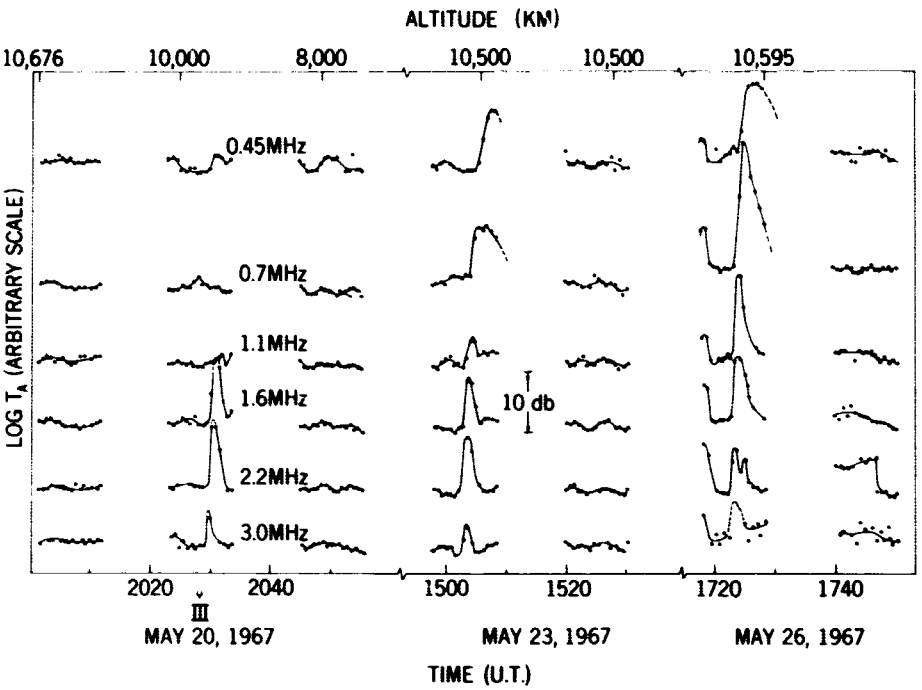
ALTITUDE (KM)
10,676
10,000
8,000
10,500
10,500
10,595
0.45MHz
0.7MHz
1.1MHz
1.6MHz
2.2MHz
3.0MHz
10 db
LOG T_A (ARBITRARY SCALE)
2020
2040
1500
1520
1720
1740
III
MAY 20, 1967
MAY 23, 1967
MAY 26, 1967
TIME (U.T.)

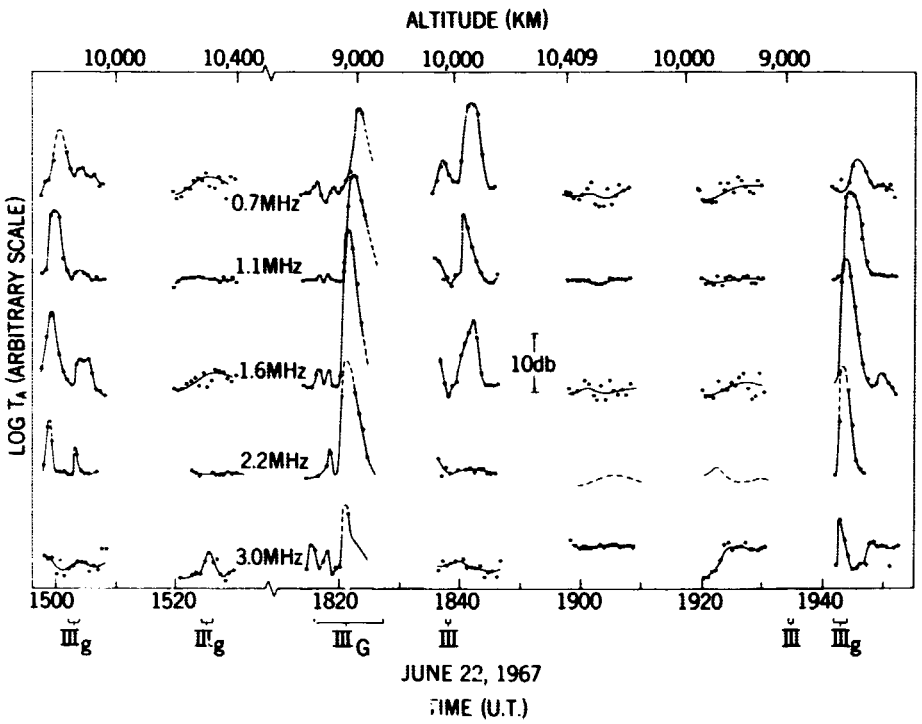
ALTITUDE (KM)
10,000
10,400
9,000
10,000
10,409
10,000
9,000
0.7MHz
1.1MHz
1.6MHz
2.2MHz
3.0MHz
10db
LOG T_A (ARBITRARY SCALE)
1500
1520
1820
1840
1900
1920
1940
III_g
III_g
III_G
III
III
III_g
JUNE 22, 1967
TIME (U.T.)

Figure 2

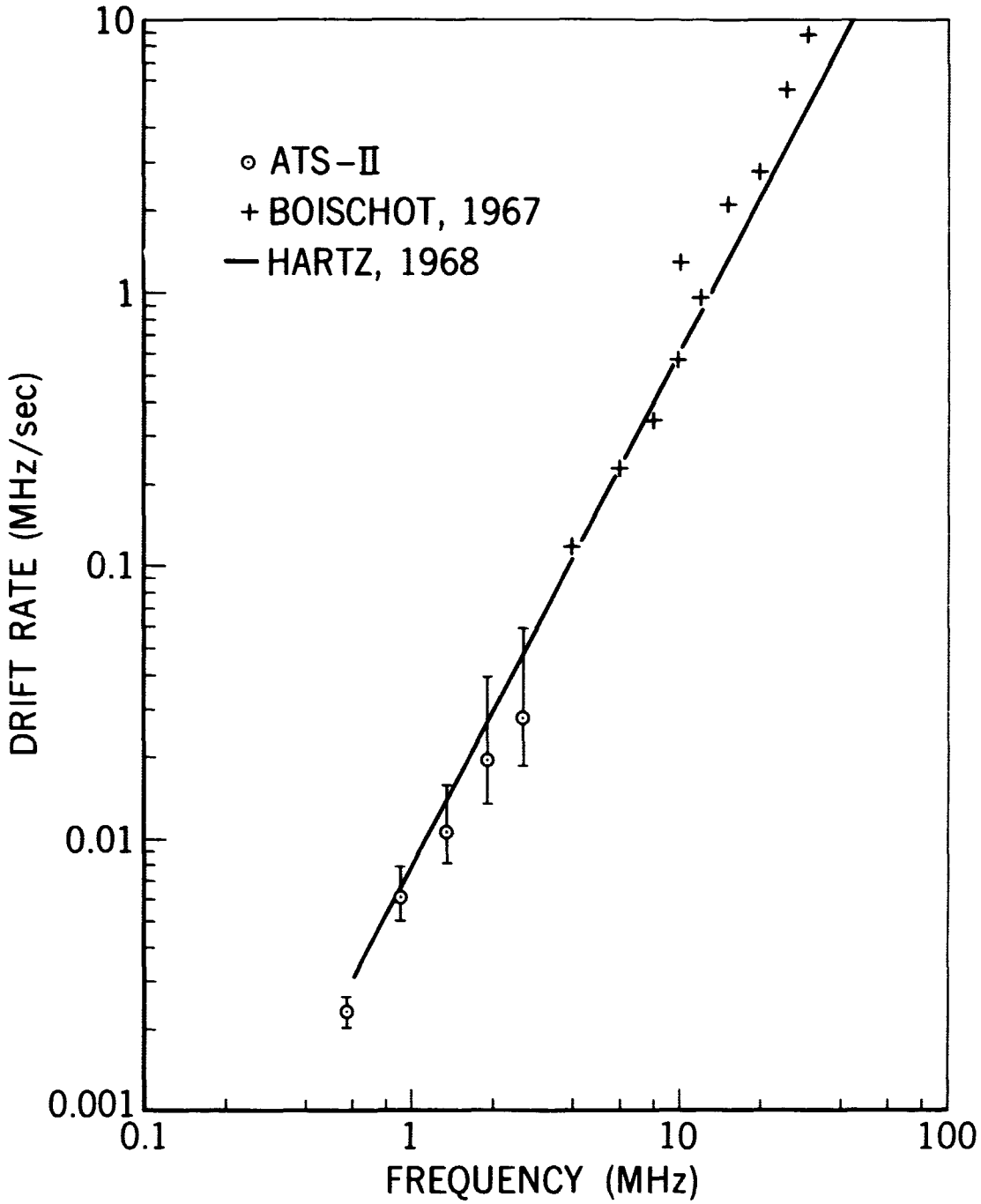
10
1
0.1
0.01
0.001
0.1
1
10
100
DRIFT RATE (MHz/sec)
FREQUENCY (MHz)
⊙ ATS-II
+ BOISCHOT, 1967
— HARTZ, 1968

Figure 3

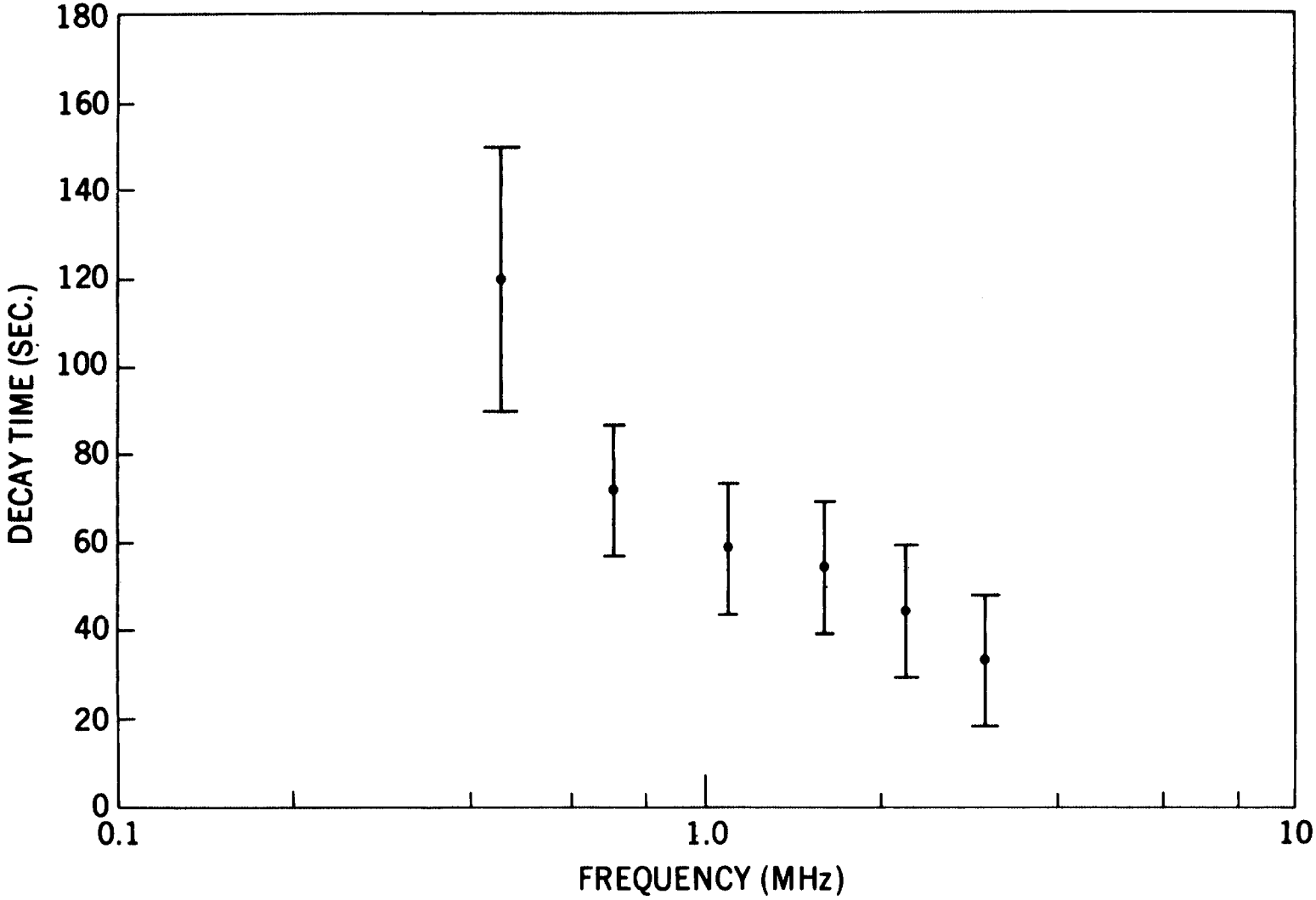
180
160
140
120
100
80
60
40
20
0
DECAY TIME (SEC.)
0.1
1.0
10
FREQUENCY (MHz)

Figure 4

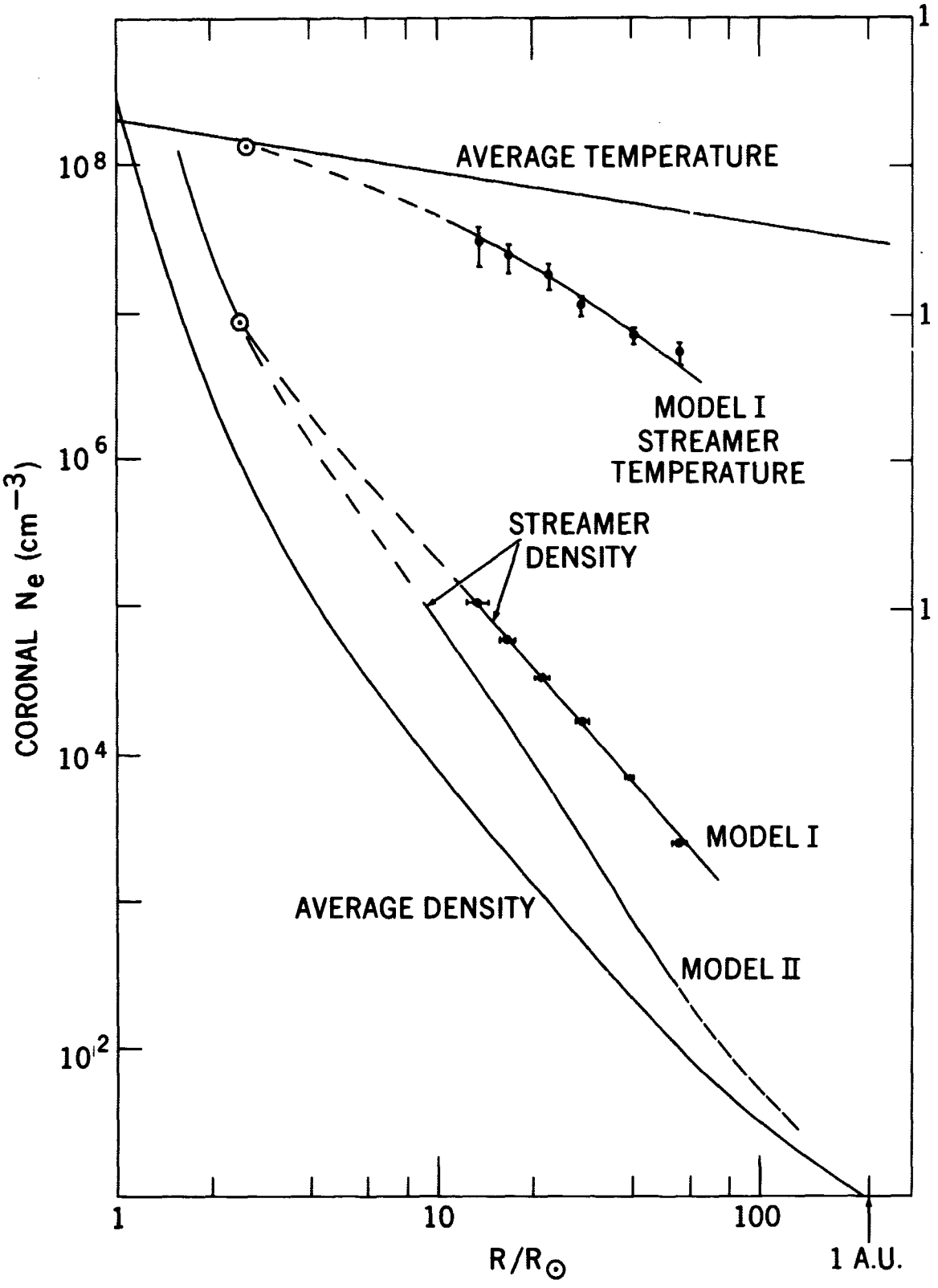
AVERAGE TEMPERATURE
MODEL I
STREAMER
TEMPERATURE
STREAMER
DENSITY
MODEL I
AVERAGE DENSITY
MODEL II
CORONAL N_e (cm^{-3})
10^8
10^6
10^4
10^2
1
10
100
$R/R_\odot$
1 A.U.
1
1
1

Figure 5

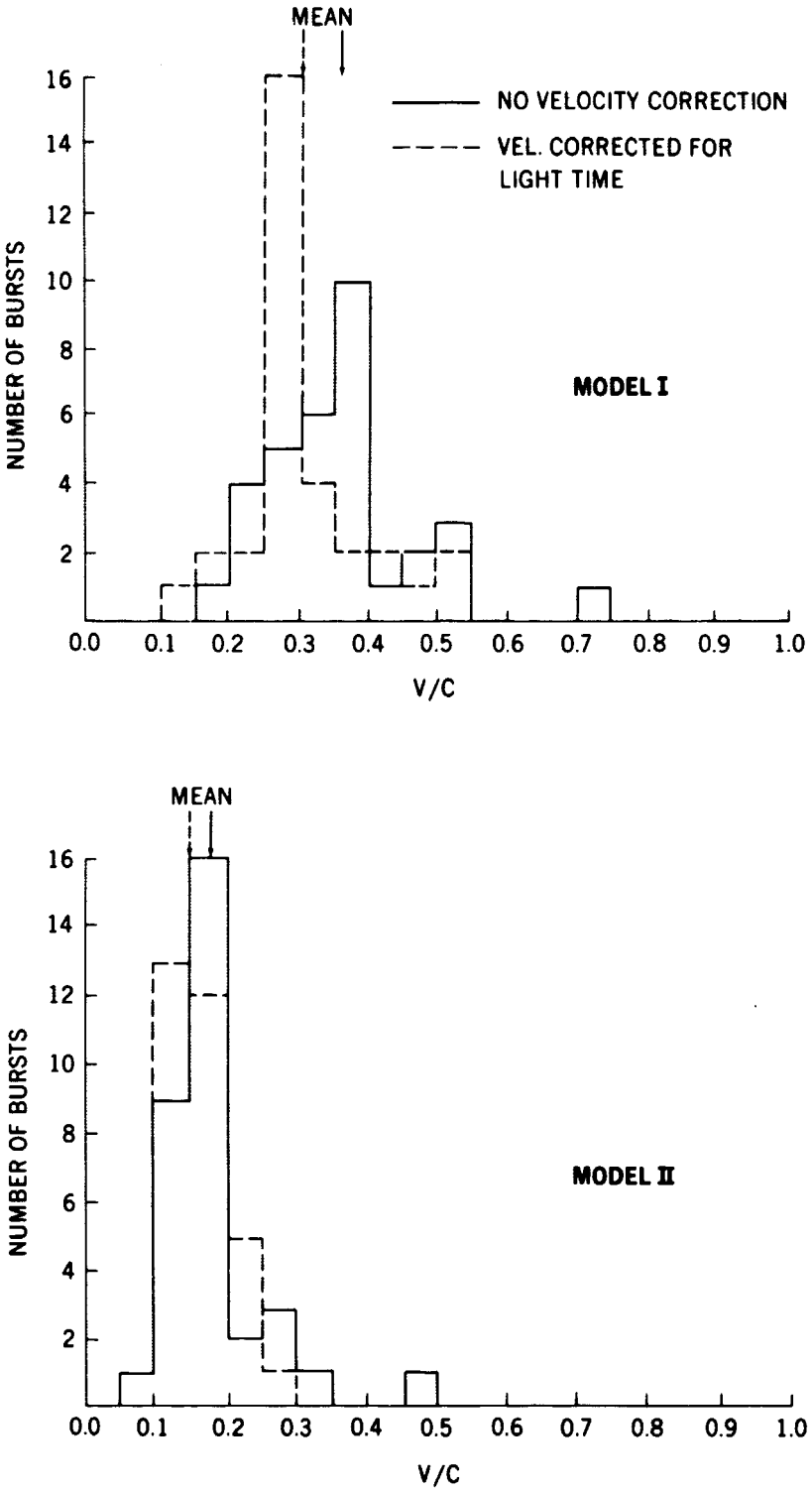
MEAN
NO VELOCITY CORRECTION
VEL. CORRECTED FOR LIGHT TIME
MODEL I
NUMBER OF BURSTS
V/C
MEAN
MODEL II
NUMBER OF BURSTS
V/C

Figure 6

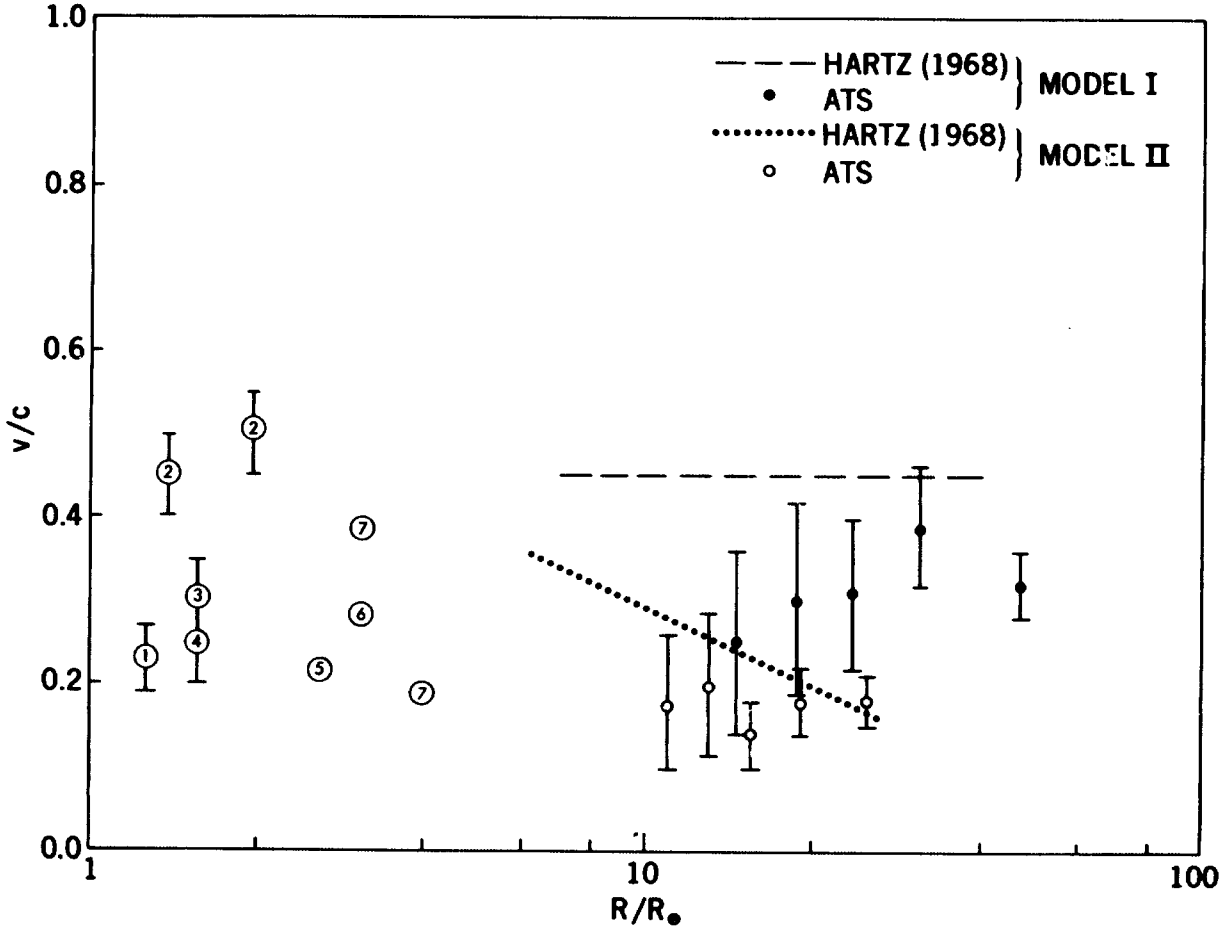
1.0
0.8
0.6
0.4
0.2
0.0
v/c
1
10
100
R/R●
HARTZ (1968)
ATS
MODEL I
HARTZ (1968)
ATS
MODEL II
①
②
②
③
④
⑤
⑥
⑦
⑦

Figure 7